The International Journal of Analytical and Experimental Modal Analysis 6(1):13–24; Jan 1991

[illegible]

by G. Prater, Jr., University of Louisville and R. Singh, The Ohio State University

ABSTRACT

This paper presents techniques that can be used to formulate, solve and interpret the complex eigenproblems associated with nonproportionally damped, longitudinally vibrating continuous rods. The formulation procedures yield none of the errors associated with discretized system approaches, and the algorithm used to solve the nonlinear eigenvalue equation is efficient and accurate. Interpretation of the system normal modes is facilitated by special complex domain normalization techniques that allow immediate assessment of the degree of nonproportionality. The concepts involved have been implemented in a computer program, and this is used to analyze example cases involving lumped and distributed viscous damping elements and various classical boundary conditions. The modal data are compared with values from a closed-form analytical solution and a lumped parameter model. Graphical results show how the eigenfunctions and eigenvalues change with increasing degrees of nonproportional damping and which parts of the system are most affected when the damper location and magnitude are changed.

1. Introduction

Modal analysis of unforced dynamic systems involves determination of normal modes, natural frequencies and damping ratios. If the damping distribution is not proportional to a linear combination of the inertia and stiffness distributions, the modes and natural frequencies will lie in the complex domain. The physical interpretation of such a solution is much different from that of an equivalent real domain solution.

While the study of nonproportionally damped discrete systems has been progressing in recent years, difficult problems involving continuous systems still remain. Distributed parameter solutions are often desirable because of modeling and accuracy constraints. The nature of discretized coordinates does not allow accurate identification of nodal points, and as we shall see, this is where the manifestations of nonproportionality in the damping distribution are most pronounced.

The purpose of this paper is to develop analytical modal analysis tools for nonproportionally damped, distributed parameter, longitudinally vibrating rods. These tools include techniques for formulating, solving and interpreting the system eigenproblem. The procedures are illustrated with three example cases and verified by comparison with results from a closed form solution and a discrete system approximation.

Glen Prater, Jr. is Assistant Professor, Department of Mechanical Engineering, University of Louisville, Louisville, KY 40292. Rajendra Singh (SEM member) is Professor, Department of Mechanical Engineering, The Ohio State University, Columbus, OH 43210.

Final manuscript received: September 26, 1990

Although the research on damped discrete systems is extensive and well documented, studies for continuous systems are limited. Distributed parameter beams and circular plates having lumped damping and stiffness elements at the boundaries have been studied by Al-Jumaily and Faulkner [1]. Criteria for approximating the system configuration by classical boundary conditions was discussed in their studies but the resulting eigenvalue problems were not solved in the complex domain. Zarek and Gibbs [2] performed a distributed parameter analysis of Euler beams with lumped impedances at the boundaries but used a numerical frequency search routine to solve the eigenvalue equation. Stevens, et al. [3] formulated the eigenproblem for a torsionally vibrating shaft with a partial damping layer but were only able to generate an approximate complex domain solution. Eigenfunction normalization proved to be a problem, with the data presented in a manner which bears little resemblance to the actual modal displacements. A method of introducing nonproportionalities which includes viscous forces as part of the boundary condition specifications has proven successful. Singh, et al. [4] used this approach for the modal analysis of a longitudinally vibrating rod. It was possible to derive a closed form eigenproblem solution for the case of a single damper, but the method does not work when applied to rods with distributed damping layers or dampers at non-boundary locations. Recently, new modeling and normalization techniques for transversely vibrating beams have been studied by Prater and Singh [5].

2. Eigenproblem Formulation and Solution

Figure 1(a) depicts a longitudinally vibrating rod having an arbitrary number of lumped viscous dampers and partial viscous damping layers. In order to specify the equation of motion, we shall divide the system into segments whose boundaries lie at lumped damper locations and at the beginning and end of distributed layers. From this definition two distinct segment types can be specified; the first is undamped along its length, and the second is completely covered by a uniform damping layer. For both segment types lumped dampers may be present at the boundaries. In this study, the rod is assumed to be slender, have uniform segment cross sections and length, and behave elasticly.

First consider an undamped segment of length, dx. Due to internal forces there are axial displacements, u, along the rod which are a function of both the position x and the time t. It is

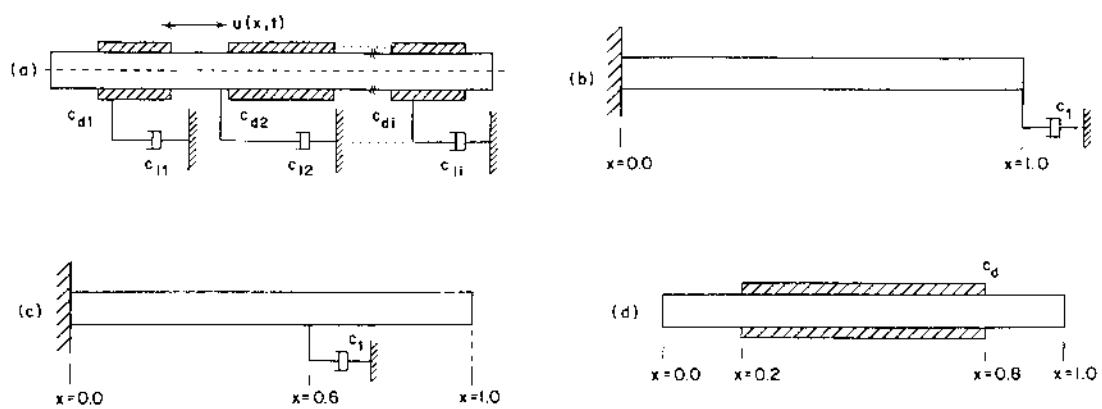

Fig. 1 (a) Longitudinally vibrating rod with arbitrary lumped and distributed viscous damping elements. (b) Example Case 1, (c) Example Case 2, and (d) Example Case 3 rod configurations

these longitudinal displacement patterns that constitute the system normal modes. If u is the displacement at x, the displacement at $x + dx$ will be $u + (\partial u/\partial x)\,dx$. The element dx in the new position will be changed in length by an amount $(\partial u/\partial x)\,dx$, and thus the unit strain is $\partial u/\partial x$. Upon using Hooke's law to relate stresses and strains and recognizing that the element acceleration is $\partial^2 u/\partial x^2$, we can write the equation of motion in dimensionless form as

$$\frac{\partial^2 u}{\partial x^2} - \alpha^2 \frac{\partial^2 u}{\partial t^2} = 0 \tag{1}$$

where dimensionless variables u, x, α, and t are defined in terms of dimensional quantities as follows:

$$\begin{aligned} u &= \bar{u}/L, \qquad x = \bar{x}/L \\ t &= \bar{t}/\tau, \qquad \alpha^2 = (L^2\rho)/(\tau^2 E g_c) \end{aligned} \tag{2}$$

Here L is the rod length, ρ is the mass per unit length, E is Young's modulus, g_c is the gravitational constant, and τ is an arbitrary time constant chosen to be one second.

When the rod segment is covered by a distributed damping layer with coefficient c_d, an axial element will be subjected to an additional force $-c_d(\partial u/\partial t)\,dx$. The equation of motion then becomes

$$\frac{\partial^2 u}{\partial x^2} - c_d \frac{\partial u}{\partial t} - \alpha^2 \frac{\partial^2 u}{\partial t^2} = 0 \tag{3}$$

Again, all quantities are unitless, and c_d is given by

$$c_d = \frac{\bar{c}_d L^2}{EA\tau} \tag{4}$$

If we denote the beginning of the i^{th} segment by x_{i1}, and the end by x_{i2}, the solution to Eqs. (1) and (3) can be written as

$$u(x,t) = \phi_{ni}(x) e^{\gamma_n t} (x_{i1} \le x \le x_{i2}) \tag{5}$$

where ϕ_{ni} is the segment eigenfunction for the n^{th} mode.

The time dependent part of the solution is the same for all segments. The constant γ is the complex natural frequency, and is given by

$$\gamma_n = -\zeta_n \omega_n \pm i\omega_n \sqrt{1 - \zeta_n^2} \tag{6}$$

where ζ is the damping ratio and ω is the undamped natural frequency.

Inserting Eq. (5) into Eq. (1) yields the following ordinary differential equation for an undamped segment

$$\frac{d^2\phi_i}{dx^2} + \alpha^2 \gamma_n^2 \phi_i(x) = 0 \tag{7}$$

Upon defining the square of the complex eigenvalue, β, as $\beta^2 = \alpha^2\gamma^2$, the general solution to Eq. (7) becomes

$$\phi_{n,i}(x) = B_{i1}\cosh\beta x + B_{i2}\sinh\beta x \tag{8}$$

where B_1 and B_2 are complex constants.

For viscously layered segments, the eigenvalue equation and eigenfunctions will be identical to those of an undamped segment having similar constraint conditions, so Eq. (8) is still valid. The eigenvalues, however, are different, and can be expressed in terms of the complex natural frequencies as

$$\beta_n^2 = \alpha^2\gamma_n^2 + c_d\gamma_n \tag{9}$$

An eigenproblem solution requires determination of the complex natural frequencies and eigenfunction coefficients, and can be accomplished by applying boundary and segment interface constraint conditions to Eq. (9). Classical fixed and free boundaries require that

$$\begin{aligned} \phi(x=b) &= 0 \qquad \text{(fixed)} \\ \frac{d\phi(x=b)}{dx} &= 0 \qquad \text{(free)} \end{aligned} \tag{10a,b}$$

If a lumped damper is present at the boundary, Eq. (10b) becomes

$$\begin{aligned} \frac{d\phi(x=b)}{dx} &= -c_l\gamma\phi(x=b) \\ c_l &= \frac{\bar{c}_l L^3}{\tau EI} \end{aligned} \tag{11}$$

At the interface between segments i and j, the constraint conditions are

$$\begin{aligned} \phi_i(x_{i2}) &= \phi_j(x_{j1}) \\ \frac{d\phi_i(x_{i2})}{dx} &= \frac{d\phi_j(x_{j1})}{dx} \end{aligned} \tag{12a,b}$$

When a lumped damper is present at the interface, Eq. (12b) becomes

$$\frac{d\phi_i(x_{i2})}{dx} + c_l\gamma\phi_i(x_{i2}) = \frac{d\phi_j(x_{j1})}{dx} \tag{13}$$

Finally, we can express the boundary and segment interface conditions in matrix form as

$$[\Psi]\{B\} = \{0\} \tag{14}$$

where $[\Psi]$ is a $4m \times 4m$ constraint matrix whose functional elements depend on γ only (m = number of rod segments), $\{B\}$ is a $4m$ column vector containing the unknown eigenfunction coefficients, and $\{0\}$ is a $4m$ null vector. Note that the lumped and distributed damping coefficients in this development can, if necessary, be replaced with arbitrary mechanical impedance elements such that

$$z_l(\gamma) = \frac{\bar{z}_l L^3}{\tau EI} \qquad z_d = \frac{\bar{z}_d L^2}{EA\tau} \tag{15}$$

An efficient algorithm for solution of Eq. (14) is developed and discussed at length in Ref. [5], but will be summarized here. The degree of coupling between the eigenfunction coefficients, the inherent nonlinearity of the boundary and constraint condition equations, and the fact that the solution lies in the complex domain all mean that a numerical approach must be used to determine γ and $\{B\}$ values. The technique used in this study involves the following steps.

Step 1. An initial guess for γ is substituted into Eq. (14).

Step 2. A series of linear transformations is used to diagonalize the constraint matrix $[\Psi]$. The final element in the last row, δ, then represents a functional value for the complex frequency equation.

Step 3. This functional value is compared to a convergence criterion and a continuation decision is made.

Step 4. If convergence is achieved, the current γ value is used in a back substitution process to determine the eigenfunction coefficients.

Step 5. If convergence is not achieved, a new γ value is computed, and steps (2) and (3) are repeated.

Steps (2) and (5) are the most critical and time consuming operations in the entire algorithm, and each requires a separate numerical technique.

3. Eigenfunction Normalization

Because the system normal modes for a nonproportionally damped system are complex values, the question of normalization arises. An obvious possibility is to divide each complex eigenfunction by the magnitude of its largest displacement. The result can then be displayed as either magnitude and phase versus x, or real part and imaginary part versus x. This approach has the appeal of simplicity and similarity to real domain techniques but, as will be seen in the example cases, is not an ideal way to present complex domain data.

We now consider a more refined scheme. Magnitudes are defined as

$$|\bar{\phi}_n(x)| = \sigma(x)|\bar{\phi}(x)| \qquad \bar{\phi}(x) = \frac{\phi(x)|\phi(x_b)|}{\phi(x_b)|\phi(x_m)|} \tag{16}$$

Here x_b is the axial location of the damping element having the largest effect on the system response and $\phi(x_m)$ is the unnormalized modal displacement with the largest magnitude. The quantity $\sigma(x)$ is a unit sign function whose value is set equal to $+1$ at $x = x_m$ and then changes sign every time the magnitude of $\phi(x)$ passes through a relative minima. The corresponding normalized phases then become

$$\theta_n(x) = \tan^{-1}\left[\frac{\mathrm{Im}(\tilde{\phi}(x))}{\mathrm{Re}(\tilde{\phi}(x))}\right] - \frac{\pi}{2}[1 - \sigma(x)] \tag{17}$$

where the branch cut in the complex plane is assumed to lie along the negative real axis. Similarly, the normalized real and imaginary parts of the eigenfunctions are given by

$$\tilde{\phi}_r(x) = \mathrm{Re}[\tilde{\phi}(x)], \qquad \tilde{\phi}_i(x) = \mathrm{Im}[\tilde{\phi}(x)] \tag{18}$$

Note that the factor of $\frac{\pi}{2}$ in Eq. (17) accounts for the sign changes induced by $\sigma(x)$ and assures that the combination of the normalized magnitude and phase represents the same complex number as is given by Eq. (18).

4. Example Case Studies

(a) Problem Formulation

First consider the system shown in Fig. 1b. This rod is fixed at $x = 0$, viscously damped at $x = 1.0$, and according to the conventions established in section 2, has one segment with constraint conditions of

$$\phi(0) = 0, \qquad \frac{d\phi(x=1)}{dx} = -c_l\gamma\phi(x=1) \tag{19a,b}$$

Applying Eq. (19a) to Eq. (8) shows that $B_1 = 0$, thus

$$\begin{aligned}[\alpha\cosh(\beta) + c_l\sinh(\beta)]\{B_2\} &= \{0\} \\ [\alpha\cosh(\beta) + c_l\sinh(\beta)] &= [\Psi]\end{aligned} \tag{20a,b}$$

The constraint derivative required in the eigenproblem solution procedure is

$$[\Psi]' = \frac{d[\Psi]}{d\gamma} = [\alpha^2\sinh(\beta) + c_l\alpha\cosh(\beta)] \tag{21}$$

Note that a closed form solution to Eq. (20a) was determined by Singh, et al. [4]. Such solutions are not possible for configurations other than one segment rods with a single lumped damper.

If the lumped damper is moved to non-boundary location $x = a$ (Fig. 1(c)), a two segment system is created. The constraint conditions then become

$$\phi_1(0) = 0$$

$$\phi_1(x=a) - \phi_2(x=a) = 0 \tag{22a, b}$$

$$\frac{d\phi_1(x=a)}{dx} + c_l\gamma\phi_1(x=a) - \frac{d\phi_2(x=a)}{dx} = 0$$

$$\frac{d\phi_2(x=1)}{dx} = 0 \tag{22c, d}$$

Finally, the viscously layered rod of Fig. 1(d) has three segments, with constraint conditions of

$$\frac{d\phi_1(x=0)}{dx} = 0$$

$$\phi_1(x=a_1) - \phi_2(x=a_1) = 0 \tag{23a,b}$$

$$\frac{d\phi_1(x=a_1)}{dx} - \frac{d\phi_2(x=a_1)}{dx} = 0$$

$$\phi_2(x=a_2) - \phi_3(x=a_2) = 0 \tag{23c,d}$$

$$\frac{d\phi_2(x=a_2)}{dx} - \frac{d\phi_3(x=a_2)}{dx} = 0$$

$$\frac{d\phi_3(x=1)}{dx} = 0 \tag{23e,f}$$

While the eigenvalues for the undamped segments are defined as before, those for the viscously damped segment are different:

$$\beta_1 = \beta_3 = \alpha\gamma, \quad \beta_2 = \sqrt{c_p\gamma + \alpha^2\gamma_2^2} \tag{24}$$

The complex natural frequencies, as system properties, are, of course, the same for each segment.

(b) Presentation and Discussion of Results

Table 1 compares Case 1 eigenvalue results ($c_l = 0.9$) with the closed form solution of Ref. [4] and with the solution for an equivalent fifteen degree-of-freedom discretized system. The current study completely agrees with the exact solution to within five significant figures. In addition, it is possible to further improve the agreement by tightening the convergence criterion of the solution algorithm. The algorithm performs efficiently; the results in the table were reached in four iterations or less. We should note that the damping value chosen for comparison, $c_l = 0.9$, lies near a singularity in the analytical solution, which further illustrates the effectiveness of the algorithm.

The discrete system eigenvalues exhibit errors that range from 7 to 36 percent. These errors are a result of the approximations inherent to a lumped parameter model. They are present even though a large model is being used and even though we are looking at only the three lowest natural frequencies. The corresponding discretized complex modes exhibit similar errors. While the discretized eigensolution is accurate enough to provide validation for our

results, the magnitude of the errors underlines the limitations of a lumped parameter model of a damped continuous system.

Figures 2-6 present, using five different approaches, the first three complex modes for Example Case 1 ($c_l = 0.9$). Figure 2 shows the modes as magnitudes and phases which have been normalized for modulus alone; Fig. 3 shows the same values when normalized using Eq. (21); Fig. 4 shows plots of the real and imaginary components; Fig. 5 shows the modes in the complex plane; and Fig. 6 illustrates the modes by plotting the instantaneous displacements (Eq. (5)) over one half cycle of motion. While these techniques yield results which are visually very different, they each depict identical complex numbers.

The simple approach of Fig. 2 has the advantage of similarity to real domain normalization techniques but yields modes which bear little resemblance to the instantaneous modal displacements of the system when it vibrates at the complex natural frequency. The method of Fig. 3, on the other hand, results in plots which are much easier to physically interpret. As the complex eigenfunction crosses the imaginary axis, a change of sign is applied to the magnitude and a 180° shift is applied to the phase. The result is exactly the same complex number but the signed magnitudes now more closely resemble the modal displacement patterns. Note that the Fig. 3 magnitudes exhibit apparent discontinuities near what were the undamped system nodal points. These are an artifact of the normalization procedure and do not represent a physical discontinuity in the rod; the eigenfunctions are continuous when viewed in the complex domain.

TABLE 1 VALIDATION OF EXAMPLE CASE 1 RESULTS

Mode	Current Study	Ref. [4]	Relative Error, %	Discrete System	Relative Error, %
		Real Part of Complex Natural Frequencies			
1	-1.4722	-1.4722	0.0000	-1.2953	12.016
2	-1.4722	-1.4722	0.0000	-1.1447	22.246
3	-1.4722	-1.4722	0.0000	-0.9595	34.825
		Imaginary Part of Complex Natural Frequencies			
1	1.5708	1.5708	0.0000	1.4388	8.4034
2	4.7124	4.7124	0.0000	4.3744	7.1726
3	7.8540	7.8540	0.0000	7.3712	6.1472
		Undamped Natural Frequencies			
1	2.1529	2.1529	0.0000	1.9360	10.075
2	4.9370	4.9370	0.0000	4.5217	8.411
3	7.9908	7.9908	0.0000	7.4333	6.980
		Damping Ratios			
1	0.68384	0.68384	0.0000	0.66908	2.158
2	0.29820	0.29820	0.0000	0.25316	15.104
3	0.18424	0.18424	0.0000	0.12908	29.939

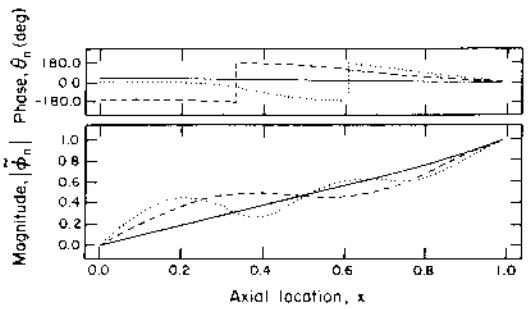

Fig. 2 Partially normalized magnitude and phase for Example Case 1 eigenfunctions, c_l = 0.9.
— Mode 1 ($\gamma_1 = -1.472 \pm 1.571i$),
- - - Mode 2 ($\gamma_2 = -1.472 \pm 4.712i$),
· · · Mode 3 ($\gamma_3 = -1.472 \pm 7.854i$)

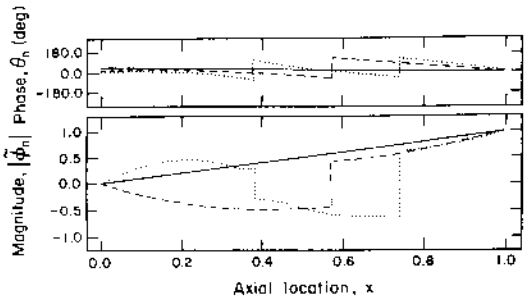

Fig. 3 Fully normalized magnitude and phase for Example Case 1 eigenfunctions, c_l = 0.9.
— Mode 1 ($\gamma_1 = -1.472 \pm 1.571i$),
- - - Mode 2 ($\gamma_2 = -1.472 \pm 4.712i$),
· · · Mode 3 ($\gamma_3 = -1.472 \pm 7.854i$)

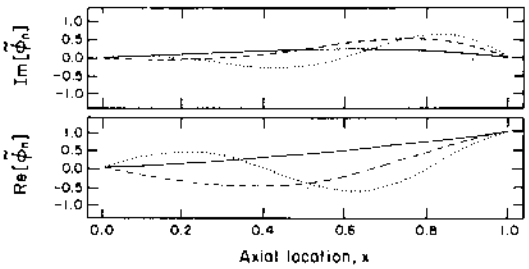

Fig. 4 Real and Imaginary parts of Example Case 1 eigenfunctions, c_l = 0.9.
— Mode 1 ($\gamma_1 = -1.472 \pm 1.571i$),
- - - Mode 2 ($\gamma_2 = -1.472 \pm 4.712i$),
· · · Mode 3 ($\gamma_3 = -1.472 \pm 7.854i$)

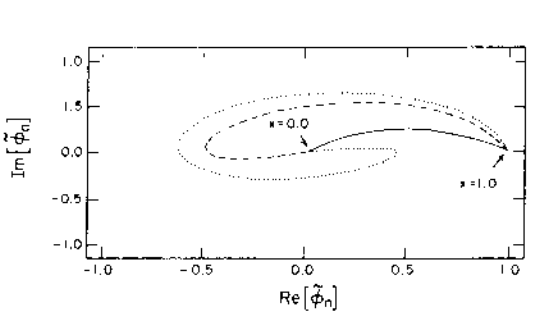

Fig. 5 Imaginary part versus real part of Example Case 1 eigenfunctions, c_l = 0.9.
— Mode 1 ($\gamma_1 = -1.472 \pm 1.571i$),
- - - Mode 2 ($\gamma_2 = -1.472 \pm 4.712i$),
· · · Mode 3 ($\gamma_3 = -1.472 \pm 7.854i$)

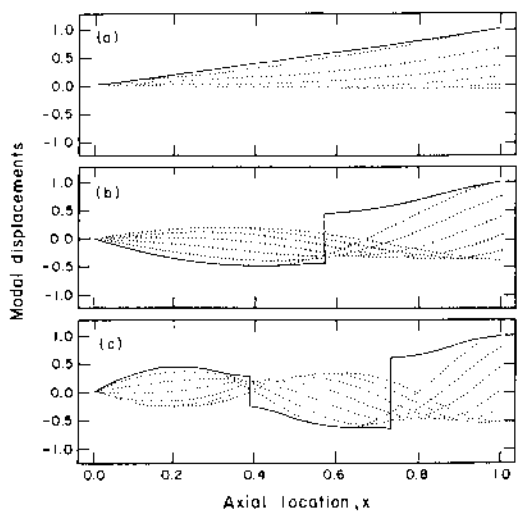

Fig. 6 Time dependent modal displacement patterns associated with Example Case 1 complex eigenfunctions, c_l = 0.9.
(a) Mode 1 ($\gamma_1 = -1.472 \pm 1.571i$),
(b) Mode 2 ($\gamma_2 = -1.472 \pm 4.712i$),
(c) Mode 3 ($\gamma_3 = -1.472 \pm 7.854i$) .
— Fully normalized magnitude,
· · · Instantaneous modal displacements

Because of interpretation difficulties, the real-imaginary plots and complex domain plots are best used as an adjunct to the other approach. They show that the imaginary parts of the modes, which are identically zero for a proportional damping configuration, are now non-zero. We see in Fig. 4 that the real part of the modes approximates the solution for the undamped case, while the imaginary part approximates the solution for the infinitely damped case.

Inspection of the instantaneous modal displacement plots of Fig. 6 shows what is perhaps the most important physical manifestation of nonproportional damping: the fact that the perfectly synchronized harmonic motion associated with real domain modes no longer exists. The non-zero phase angles of the complex modes indicate relative longitudinal motion along the rod. This means that true nodal points are no longer present and that when the displacement of a specific point reaches a relative maxima (with corresponding zero velocity), other points are still moving. This figure further illustrates the utility of the Eq. (16) normalization scheme. The normalized magnitude resembles the modal displacement pattern, even for this highly nonproportional case. With slightly nonproportional damping configurations, the resemblance is even more pronounced.

Figure 7 plots the system damping ratios versus damping coefficient. As the coefficient increases, the damping ratios increase, until they reach a maximum at $c_l = 1.0$. When the coefficient is further increased, the damper begins behaving like a fixed boundary, less energy is dissipated, and the damping ratio decreases.

Figure 8 presents a plot of the maximum magnitude discontinuity as a function of the damping coefficient. It shows that the discontinuities of modes 2 and 3 increase to a well defined maximum (except for the singularity at $c_l = 1.0$) and then decrease, eventually back to zero (infinite damping, another proportional damping configuration). There are no discontinuities for mode 1 because it has no undamped nodal points. In fact, in-phase modes are inevitably less affected by damping nonproportionalities than out-of-phase modes.

The ratio of the maximum imaginary part of the eigenfunction to the maximum real part is shown in Fig. 9. The value increases in a linear fashion from a value of zero at $c_l = 0.0$. A ratio of 1.0 represents the most heavily nonproportional configuration possible; as the value increases beyond 1.0, the nonproportionality begins to decrease as the damping element begins to behave like a fixed support. The magnitude discontinuities and imaginary/real ratio have been suggested for use as numerical indices for quantifying the extent of nonproportionality in the damping distribution [5].

Typical Case 2 eigenfunction plots are presented in Fig. 10. Those shown here correspond to a configuration with a lumped damper of strength $c_l = 3.6$ located at $x = 0.6$. While the results are generally similar to those of Case 1, two important differences are apparent. The effect of the damping element, in terms of energy dissipation and nonproportionality, is highly

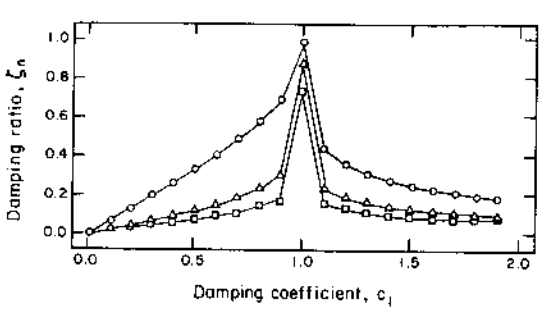

Fig. 7 Damping ratio versus nondimensional damping coefficient, Example Case 1.
○—○ **Mode 1,** △—△ **Mode 2,** □—□ **Mode 3**

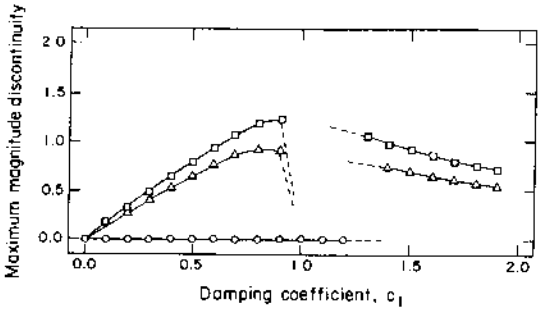

Fig. 8 Maximum magnitude discontinuity versus nondimensional damping coefficient, Example Case 1.
○—○ **Mode 1,** △—△ **Mode 2,** □—□ **Mode 3**

dependent on the location of the damper relative to nodal points. When the element is near an undamped nodal point, it will have little effect on that particular mode. If it lies near a point of large modal displacement, energy dissipation and manifestations of nonproportionality will be maximized. In this instance the damper is situated near a mode 2 undamped node; consequently, the damping ratio and nonproportionality are quite small. The effect on mode 3, with an anti-node near the damper, is much more pronounced.

A second characteristic of non-boundary damping elements is that there is a discontinuity in the slope of modes at the damper location. This is apparent in both the eigenfunction magnitudes and instantaneous modal displacements (Fig. 11). Such behavior is explained by inspection of constraint equation (22c). This expression represents a force balance at the damper location, and involves the internal axial forces in the respective rod segments and the damper force. The internal forces are unequal and proportional to the strain, $\partial u/\partial x$, hence a slope discontinuity develops.

Figure 12 presents a representative set of eigenfunctions for Case 3. Here the viscous damping layer has a coefficient of $c_d = 3.6$, begins at $x = 0.20$, and ends at $x = 0.80$. We see the same manifestations of nonproportionality as in the first two cases, with the exception that no strain discontinuities exist at the layer edge.

5. Concluding Remarks

The numerical solution algorithm performed effectively for each of the example cases. Even though an extremely small convergence criterion (1.0E-8) was specified, solutions were achieved within two to seven iterations. The algorithm has been proven to work with systems governed by the Euler equation [5], and will work equally well with other wave equation systems such as transversely vibrating strings and torsionally vibrating shafts.

Our study has highlighted the most important physical manifestation of nonproportional damping: the non-synchronous motion which occurs when the system vibrates at a natural frequency. This type of motion is strikingly different from the in-phase motion associated with undamped or proportionally damped modes. The differences are so pronounced that traditional experimental modal analysis techniques may yield suspicious results when applied to heavily nonproportional systems. These observations are important when considered in light of the

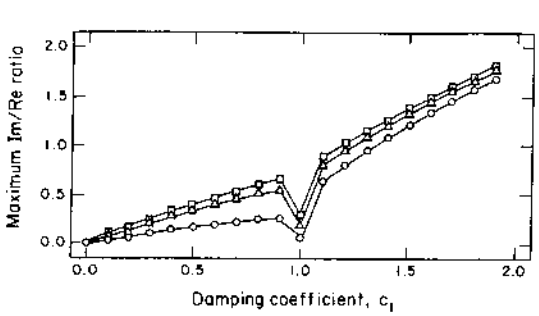

Fig. 9 Maximum imaginary/real ratio versus nondimensional damping coefficient, Example Case 1.
○—○ Mode 1, △—△ Mode 2, □—□ Mode 3

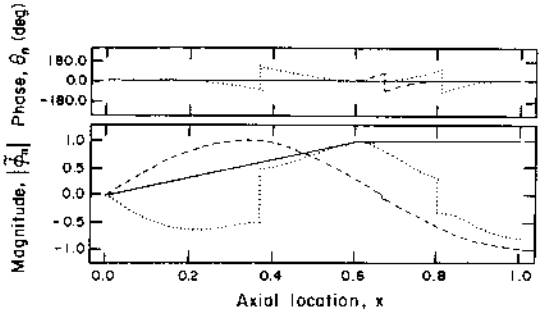

Fig. 10 Fully normalized magnitude and phase for Example Case 2 eigenfunctions, c_l = 1.4.
— Mode 1 ($\gamma_1 = -1.019 \pm 1.406i$),
--- Mode 2 ($\gamma_2 = -0.1281 \pm 4.723i$),
··· Mode 3 ($\gamma_3 = -1.583 \pm 7.854i$)

fact that a proportional damping approximation is a very restrictive assumption. If a system is damped, it is likely to be nonproportionally damped, especially if the damping effect is localized, or if the structure is irregular enough that stiffness and inertia concentrations exist. The indices discussed here provide a means of assessing the extent of nonproportionality and selecting an appropriate analysis approach.

Finally, this work provides analysis tools that can be used to optimize damping treatments for noise and vibration control. Comparison of the results from the example cases clearly shows that the effectiveness of a damping element, whether it is lumped or distributed, depends on both its magnitude and its location relative to the system nodal points. We are now in the process of developing dimensionless design charts for various system types to better quantify this behavior.

References

1. Al-Jumaily, A.; Faulkner, L. "Vibration of continuous systems with compliant boundaries." *J Sound Vib* v 54 p 203-213 1977.
2. Zarek, J.; Gibbs, B. "The derivation of eigenvalues and mode shapes for the bending motion of a damped beam with general end conditions." *J Sound Vib* v 78 p 185-196 1985.
3. Stevens, K.; Martinez, M.; Kelly, W. "A comparison of exact and approximate methods of analysis for added viscoelastic damping treatments." *Proceedings of the 6th International Modal Analysis Conference*, Kissimmee, FL, Feb 1-4, 1988. v 2 p 1602-1608
4. Singh, R.; Lyons, W.M.; Prater, G. "Complex eigensolution for longitudinally vibrating bars with a viscously damped boundary." *J Sound Vib* v 133 p 364-367 1989.
5. Prater, G.; Singh, R. "Eigenproblem formulation, solution, and interpretation for nonproportionally damped beams." *J Sound Vib* v 141 p 125-142 1990.

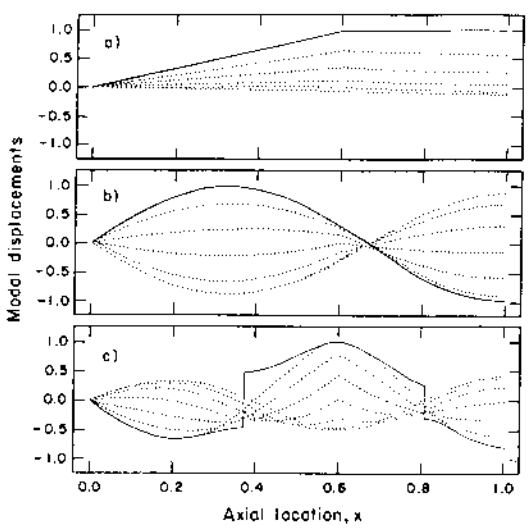

Fig. 11 Time dependent modal displacement patterns associated with Example Case 2 complex eigenfunctions, $c_l = 1.4$.
(a) Mode 1 ($\gamma_1 = -1.019 \pm 1.406i$),
(b) Mode 2 ($\gamma_2 = -0.1281 \pm 4.723i$),
(c) Mode 3 ($\gamma_3 = -1.583 \pm 7.854i$)
— Fully normalized magnitude,
··· Instantaneous modal displacements

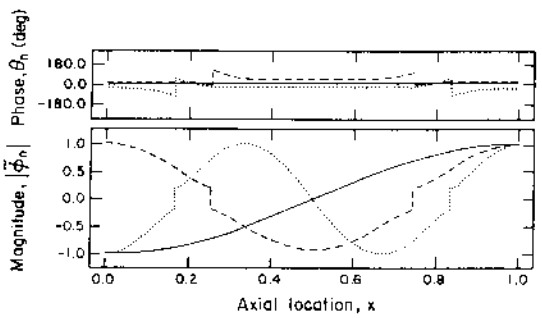

Fig. 12 Fully normalized magnitude and phase for Example Case 3 eigenfunctions, $c_l = 3.6$.
— Mode 1 ($\gamma_1 = -0.5477 \pm 3.137i$),
- - - Mode 2 ($\gamma_2 = -0.8443 \pm 6.059i$),
··· Mode 3 ($\gamma_3 = -1.186 \pm 9.245i$)